Synthesis, structure and reactions of 1-(p-chlorophenyl)-3-(2,4,6-tri-t-butylphenyl)-1-aza-3-phospha-allene

Xi-Geng Zhou [a,*], Li-Bei Zhang [a], Rui-Fang Cai [a], Qiang-Jin Wu [b], Lin-Hong Weng [c], Zu-En Huang [a]

[a] Department of Chemistry, Fudan University, Shanghai 200433, People's Republic of China
[b] The State Key Laboratory of Structural Chemistry, Fuzhou 350002, People's Republic of China
[c] The State Key Laboratory of Elemental Organic Chemistry, Tianjin 300071, People's Republic of China

Abstract

A new phosphaazaallene Mes*P=C=NAr (Mes* = 2,4,6-^{t}Bu$_3$C$_6$H$_2$, Ar = p-ClC$_6$H$_4$) (1) has been synthesized. Complex 1 reacts with Mes*PHSiMe$_2^t$Bu to form the phosphaazaallene insertion product Mes*P=C(PHMes*)NAr(SiMe$_2^t$Bu) (2). The treatment of 1 with an excess amount of YCl$_3$ in THF leads to the isolation of the symmetrical dimer Mes*P(μ-CNAr)$_2$PMes* (3), indicating both of the P=C and C=N bonds of 1 are reactive sites. X-ray structure analysis of 1 indicates that the distance of the P=C bond, 1.642(5) Å, is markedly shorter than those of isolated P=C bonds (1.66–1.72 Å), and the N=C=P unit slightly deviates from linearity with the P=C=N angle of 170.8(4)°. The structure determination of 2 revealed the molecule adopts a planar conformation about P=C bond and the mutual orientation of two bulky Mes* moieties is almost orthogonal (92.8°). Complex 3 is a symmetrical four-membered ring structure in which the Mes* rings lie nearly perpendicular to the planes of the Ar ring and the P$_2$C$_2$ ring (84.8 and 75.6°, respectively), while the Ar ring is almost parallel to the plane of the P$_2$C$_2$ ring (25.2°). © 2000 Elsevier Science S.A. All rights reserved.

1. Introduction

There has been much recent interest in phosphacumulenes because of their moiety of ambident reactives as well as their unique bonding situation [1–10]. The heteropolar addition of an organometallic reagent to the double bond of unsaturated molecules is the simplest manifestation pattern. Varieties of insertion reactions for other heterocumulenes such as carbon dioxide, carbodiimides, isocyanates, isothiocyanates, carbon disulfide, etc. have been known [11–14]. In contrast, although isoelectronic phosphacumulenes are thought desirable to possess some reactivities similar to their nitrogen analogues, their reactivities have been studied to a lesser extent due to the starting late and the difficulty of preparation. Only a few examples of insertions have been described so far [8,10,15,16], it is still uncertain whether the phosphaazaallenes can become excellent building blocks in organic and organometallic synthesis as imines, phosphaalkenes or carbodiimides featuring. On the other hand, since π bonding is generally weakened with increasing atomic number, for phosphaazaallene-type compounds most of reactions reported occur at the site of P=C double bond to date [3–8], their reactivities at the C=N bond are relatively unexplored [9,10]. In order to explore the cooperative reactivity of different polar cumulative double bond units, we report here the synthesis and reactivities of a new phosphacumulene Mes*P=C=NAr.

2. Results and discussion

2.1. Synthesis of Mes*P=C=NAr (1)

We have synthesized the new phosphaazaallene Mes*P=C=NAr (1) by a slightly modified literature

* Corresponding author. Tel.: + 86-21-65643885; fax: + 86-21-65641740.
E-mail address: xgzhou@fudan.edu.cn (X.-G. Zhou).

method for reactivity studies [3,17]. There have been several reports on the preparation of phosphaazaallenes, in which all the products were column chromatographed over silica gel. However, compound **1** decomposes very easily in the same conditions of the column chromatography due to more highly reactive and sensitive to moisture. Therefore, for the purification of **1** the recrystallization is a preferable method to the column chromatography. It needs to point out that when **1** is purified by the extraction and recrystallization with *n*-hexane, the stoichiometric reactions must be strictly controlled and the THF solvent must be completely removed from the residue, if not, **1** will be very difficult to isolate.

Compound **1** was characterized by IR, ^{1}H-NMR, UV, and mass spectroscopies. The IR spectrum of **1** shows the characteristic absorption of the asymmetric stretching vibration of the P=C=N moiety at 1831 cm^{-1} is lower, by about 15 cm^{-1}, than the corresponding absorption of Mes*P=C=NPh due to the far conjugation of the chlorine atom. The molecular ion and main fragments are clearly observed in the mass spectra, indicating **1** to be monomeric structure.
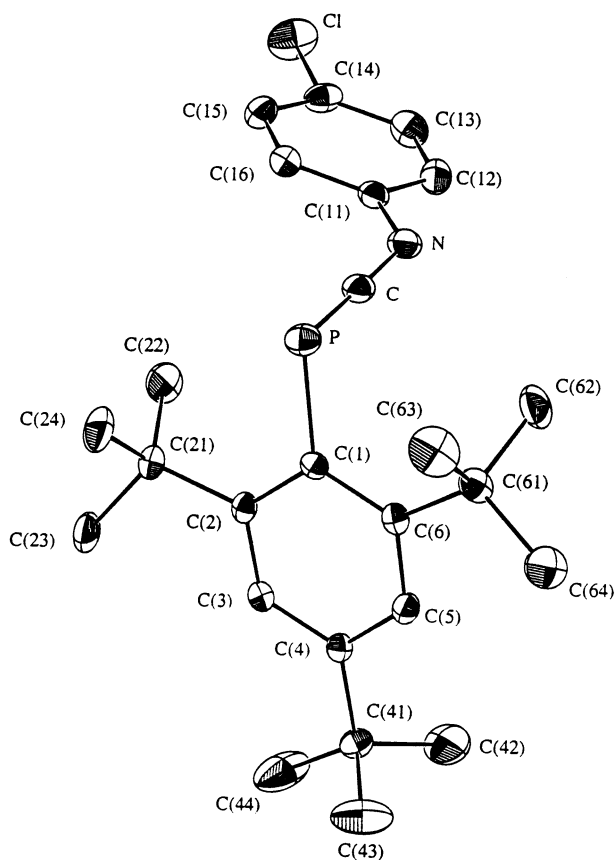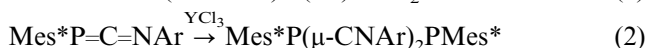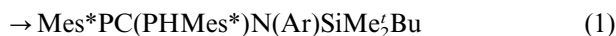

Fig. 1. Molecular structure of Mes*P=C=NAr (**1**). Selected bond lengths (Å) and angles (°): P–C 1.642(5), P–C(1) 1.860(4), N–C 1.214(6), N–C(11) 1.423(6), Cl–C(14) 1.732(5); C–P–C(1) 99.8(2), C–N–C(11) 128.3(4), N–C–P 170.8(4).

2.2. Crystal structure of Mes*P=C=NAr (1)

The X-ray structure of **1** is shown in Fig. 1, with selected bond lengths and angles in the caption. The P, C, N and C(11) atoms are coplanar within 0.03 Å. The interplanar angle between this plane[P, C, N and C(11)] with the Ar ring is 16.4°, which is remarkably smaller than that found in Mes*P=C=NPh, 22.7°. The change of the orientation of the Ar ring relative to the P=C=N–C(11) plane suggests that some far conjugation may be taking place between the cumulene chain and the chlorine atom of the Ar group [18]. The C(1), P, C and N atoms are also coplanar within 0.02 Å. This plane[C(1), P, C, N] makes an angle of 77.2° with the plane of P, C, N and C(11) atoms, and makes an angle of 85.4° with the Mes* ring. These values are respectively similar to the corresponding dihedral angles in Mes*P=C=NPh, 75.8 and 87.4°. The P=C distance of 1.642(5) Å in **1** is comparable to the values found in other phosphacumulenes, such as Mes*P=C=NPh, 1.651 Å [19] and Mes*P=C=PMes*, 1.635(8) Å [20], but is markedly shorter than isolated P=C bond distances with an sp^2-hybridized C atom (1.66–1.72 Å) [21,22]. This shortening presumably results from the special electronic characteristics of heteroallene system and the smaller bond radius of the sp-hybridized C atom. The C=N distance [1.214(6) Å] is in the normal range observed for carbodiimide systems [18], and is similar to that observed in Mes*P=C=NPh (1.209 Å) [19]. The ring plane of Mes* group is almost perpendicular to that of the Ar group, probably due to the steric repulsion of the Ar group and the *ortho-t*-butyl groups of the Mes* group.

The P=C=N angle of 170.8° in **1** is smaller than the value expected for linear allene molecule which is probably due to packing forces as commonly found in cumulenes. The C(1)–P–C angle of 99.8° is similar to those in Mes*P=CPh$_2$ [22] and 1,3-diphosphaallene [20]. The smaller angle at the central P atom parallels also those found in dipnictene compounds, such as diphosphenes, diarsene, distibene and dibismuthene. As a result it has been proposed that since the s-orbital character of the lone pairs increases with increasing atomic number, the pnictogen atom trends toward bonding to substituent via one non-hybridization p-orbital, thus the angle at the pnictogen atom decreases sequentially from phosphorus to bismuth [23–27]. Interestingly, it is contrasted with the main trend of decrease observed in the heavier pntictogen congeners, the C–N–C(11) angle (128.3°) is significantly larger than that in PhN=NPh (N–N–C = 113.6°) [28], and is even wider than that expected for the sp^2 hybridization angle. This is probably a result of the greater steric

congestion as well as the lone pair in the p-orbital for the smaller, lighter nitrogen atom.

2.3. Studies on reactivity of Mes*P=C=NAr (1)

Compound **1** reacts with Mes*PHSiMe$_2^t$Bu to form the phosphaazaallene insertion product Mes*P=C(PHMes*)NAr(SiMe$_2^t$Bu) (**2**) with migration of phosphinyl onto the central carbon atom of phosphaazaallene to form phosphaalkene (Eq. (1)). In contrast to the results of the unsymmetrical dimerization of Mes*P=C=NPh, catalyzed by Pd(0) complexes [9], YCl$_3$ catalyzes dimerization of **1** to yield the symmetrical dimer Mes*P(μ-CNAr)$_2$PMes* (**3**) (Eq. (2)). This reaction proceeds smoothly regardless of the polarity of solvents at room temperature, and is irreversible under the mild reaction conditions. Related dimerization has been previously observed [9,29], and has been attributed to [2 + 2]-cycloaddition at the P=C double bond. Two bands of strong to medium intensity in the range of 1521–1591 cm^{-1} are attributed to the symmetric and antisymmetric C=N stretches of the 2,4-diimino-1,3-diphosphetanes.

Mes*PCNAr + Mes*PHSiMe$_2^t$Bu

$\rightarrow$ Mes*PC(PHMes*)N(Ar)SiMe$_2^t$Bu   (1)

Mes*P=C=NAr $\xrightarrow{\text{YCl}_3}$ Mes*P(μ-CNAr)$_2$PMes*   (2)

Since insertion of a small molecule or an organic functional group into a metal–carbon bond represents a fundamental step for any metal-promoted functionalization of a hydrocarbon residue, there is currently considerable interest in studying the reactivities of the Ln–C bonds of organolanthanide complexes. Varieties of the Ln–C bond insertion reactions for other isoelectronic heterocumulenes such as carbon dioxide, isocyanates, carbon disulfide, etc. have been known [30,31]. However, no insertion of phosphacumulenes into the Ln–C bond has been described up to now. To further understand if Mes*P=C=NAr is capable of undergoing the same insertion reaction, we studied the reaction of **1** and (C$_5$H$_4$Me)$_2$Dy(CMe$_3$), but the result indicates that **1** can not be inserted into the Dy–C bond at room temperature. This may be due to that the steric factor of (C$_5$H$_4$Me)$_2$Dy(CMe$_3$) is unfavorable to the bulky **1** to attack at the Dy–C bond.

The formations of **2** and **3** indicate that both the P=C and C=N bonds of **1** are reactive sites, and the reaction selectivity depends to a large extent on the steric factors and the electronic effects. Many previous investigation results indicate that the P=C site is more reactive than the C=N one in the phosphaazaallene molecules, and the polarity of the P=C bond might be the phosphorus atom as the more positive partner. It is probably the steric hindrance that makes the most important contribution to the low reactive imine insertion into the P–Si

bond instead of the high reactive phosphaalkene one. Because the two bulky ortho-t-butyl groups cause the very large steric hindrance around the P=C and P–Si units, this is unfavorable to their mutual action. As a result, it provides a competitive chance for the smaller steric hindrance C=N bond to react with Mes*PHSiMe$_2^t$Bu. Although the insertions of other cumulenes (e.g. RN=C=NR′, CS$_2$, PhN=C=O, etc.) into P–Si bond have been known for long time, few insertions of phosphaazaallenes into P–Si are reported [10]. This may give a new insight into the reactivity of phosphacumulenes. Thus, further studies on other insertions of phosphacumulenes are currently under way.

2.4. Description and discussion of crystal structure of 2

The crystal structure of **2** (Fig. 2) shows that the molecule adopts a planar conformation about P=C bond containing the atoms C(2), P(1), C(1), N and P(2), and the N atom is in a sp^2 hybridization state with ΣN = 360°. But the P(2) center has quite pyramidal coordination, ΣP = 290.5°, suggesting little delocalization of the P(2) lone pair, at least in the ground state [32,33]. To release the steric congestion between two extremely bulky 2,4,6-^{t}Bu$_3$C$_6$H$_2$ moieties, their mutual orientation is almost orthogonal (92.8°). In addition, the plane comprising from P(1), C(1), P(2) and N also lies nearly perpendicular to three aromatic ring planes, and made dihedral angles with planes of C(2)–C(7) ring, 77.8; C(20)–C(25) ring, 90.7 and C(44)–C(49) ring, 84.6°, respectively. The C(1)–P–C(2) angle [112.6(2)°] is significantly wider than that in **1**, 99.8°. This is probably a result of the greater steric crowding arising from the additional bulky Mes*PH and SiMe$_2^t$Bu substituents compared with **1**. The P(1)–C(1) distance of 1.701(4)Å is in normal range observed for isolated P=C double bond distances [21,22]. Comparison of P–C distances in **1** and **2**, it is found that the P–C distance changes with the difference of the carbon hybridization states, but hardly changes with the difference of the phosphorus ones. The coordination environment about the silicon atom is approximately tetrahedral.

2.5. Description of crystal structure of 3

The structure of **3** is similar to those of RP(μ-C=NPh)$_2$PR [R = CH$_2$CH$_3$, CH$_2$Ph, 2,4,6-(^{t}Bu)$_3$C$_6$H$_2$] [9,29]. The four-membered ring P$_2$C$_2$ is a planar and has a rhombic geometry with the P–C bond distances [1.813(2) and 1.829(2) Å] and the P–C–P and C–P–C bond angles [94.5(1) and 85.5(1)°, respectively]. The Mes* rings lie nearly perpendicular to the planes of the Ar ring and the P$_2$C$_2$ ring (84.8 and 75.6°, respectively), while the Ar ring is almost parallel to the plane of the P$_2$C$_2$ ring (25.2°). The average P–C bond distance of
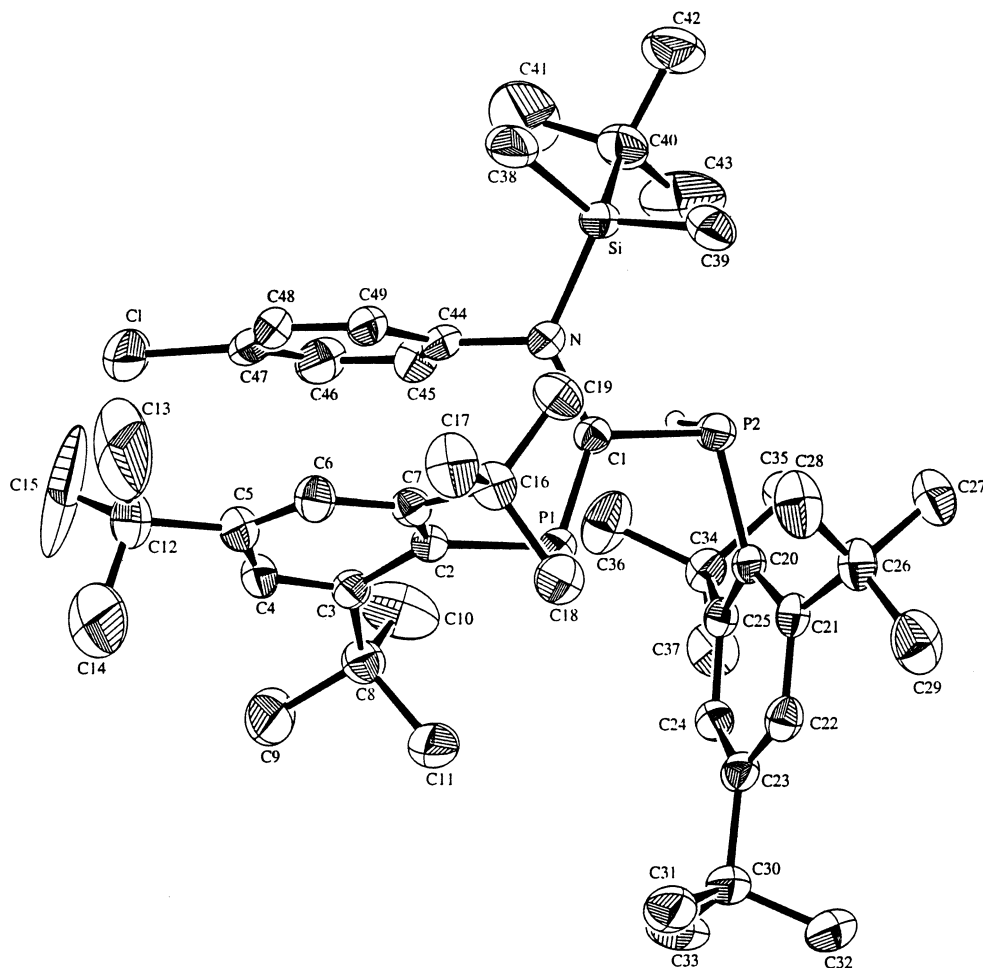
Fig. 2. Molecular structure of Mes*P=C(PHMes*)NAr(SiMe$_2^t$Bu) (**2**). Selected bond lengths (Å) and angles (°): P(1)–C(1) 1.701(4), P(1)–C(2) 1.872(4), P(2)–C(1) 1.868(4), P(2)–C(20) 1.856(4), N–C(1) 1.432(4), N–C(44) 1.444(4), Si–N 1.783(3), Si–C(38) 1.860(5), Si–C(39) 1.842(5), Si–C(40) 1.901(5), C(1)–P(1)–C(2) 112.6(2), C(1)–P(2)–C(20) 104.8(2), P(1)–C(1)–P(2) 115.1(2), P(1)–C(1)–N 133.5(3), P(2)–C(1)–N 111.4(2), C(1)–N–C(44) 115.0(3), C(1)–N–Si 128.4(2), C(44)–N–Si 116.6(2).

1.821(2) Å in the ring is comparable to the exocyclic P–C bond distance of 1.845(2) Å. The C=N bond distance of 1.282(3) Å is similar to the values observed previously. The steric constraints imposed by the Mes* groups require them to be trans each other and the Ar groups to adopt the Z-configuration. The endocyclic angle of 85.5° at phosphorus atom is markedly widened as compared to the corresponding angles in [CH$_3$CH$_2$P(μ-CNPh)]$_2$ and [PhCH$_2$P(μ-CNPh)]$_2$ [81 and 82°, respectively], but the endocyclic angle at carbon atom is smaller than the values observed in the above compounds, 99 and 98°. This is presumably due to the increased steric demand of the supermesityl group as compared to CH$_3$CH$_2$- and PhCH$_2$-groups.

3. Experimental

All the manipulations were carried out under purified argon using Schlenk technique. THF and *n*-hexane were refluxed and distilled over sodium benzophenone ketyl immediately before use. 2,4,6-Tri-*t*-butylphenylphosphine (Mes*PH$_2$) was prepared by the published procedure [34]. *t*-Butylchlorodimethysilane (Aldrich) was purified by sublimation prior to use. The Mes*PHSiMe$_2^t$Bu was prepared by reaction of equiv of Mes*PH$_2$ and BuLi in THF, followed silylation with Me$_2^t$BuSiCl. Elemental analyses for C, H and N were carried out on a Perkin–Elmer 240C analyzer. Infrared spectra were obtained on a Nicolet FT-IR 360 spectrometer. A Nujol mull of the compound was pressed between KBr pellets. Mass spectra were recorded on a HP 5989A instrument operating in EI mode. Samples were introduced by direct probe inlet without any heating. The ion source temperature was 200°C. UV–visible spectra were recorded on a HP 8452A UV–vis absorption spectrophotometer. ^{1}H-NMR data were obtained on a Bruker MSL-300 NMR spectrometer.

3.1. Preparation of 1-(p-chlorophenyl)-3-(2,4,6-tri-t-butylphenyl)-1-aza-3-phospha-allene (1)

Addition of butyllithium (1.80 M, in cyclohexane, 1.80 ml) to a stirred solution of 2,4,6-tri-t-butylphenylphosphine (0.900 g, 3.24 mmol) in 60 ml of THF at $-50°C$ caused an red solution under argon. After 3 h, to the reaction solution t-butyl-chlorodimethylsilane (0.490 g, 3.25 mmol) was added at $-15°C$. The clear red solution became immediately pale. Then, butyllithium was added to the mixture (3.25 mol) at $-10°C$. After being stirred overnight at ambient temperature, the reaction mixture was cooled at $-50°C$ and was slowly added to a cooled ($-50°C$) solution of 4-chlorophenyl isocyanate (0.50 g, 3.26 mmol) in THF (20 ml) to give a red solution. After being stirred for 3 h at $-50°C$, the reaction mixture was warmed up to ambient temperature. The solvent was evaporated under vacuum, and the yellow solid was extracted with 100 ml of hexane. The red extract solution was concentrated and cooled at $-30°C$ to give an orange–yellow powder. Recrystallization of the orange–yellow powder from hexane gave 1 as orange crystals (0.325 g, 24%). M.p. 148–149°C. ^{1}H-NMR (CDCl$_3$): δ = 7.43 (d, ${}^4J_{PH}$ = 2.3 Hz, 2H, m-Mes*), 7.09–7.28 (m, 4H, Ar), 1.66 (s, 18H, o-^{t}Bu), 1.30 (s, 9H, p-^{t}Bu). IR (KBr, cm^{-1}): 3395 w, 2960 s, 2862 s, 1831 m, 1700 w, 1593 w, 1585 w, 1572 w, 1482 s, 1467 s, 1377 m, 1240 w, 1204 w, 1091 m, 1012 m, 878 m, 832 s, 742 m. UV (hexane): λ_{max} 220 (ε 18 100), 268 (23 900), 296 (sh 8180), 420 nm (430). MS (EI): m/z (fragment, relative intensity) = 413 [M$^+$, 65], 356

Fig. 3. Molecular structure of Mes*P(μ-CNPh)$_2$PMes*. Selected bond lengths (Å) and angles (°): P(1)–C(1) 1.829(2), P(1)–C(1A) 1.813(2), P(1)–C(31) 1.845(2), P(1)–P(1A) 2.674(1), Cl(1)–C(24) 1.741(3), N(1)–C(1) 1.282(3), N(1)–C(21) 1.405(3), C(1)–P–C(1A) 85.5(1), C(1)–P–C(31) 122.2(1), C(1A)–P–C(31) 121.9(1), C(1)–N(1)–C(21) 124.8(2), N(1)–C(1)–P(1) 139.3(2), N(1)–C(1)–P(1A) 125.8(2), P(1)–C(1)–P(1A) 94.5(1).

[M$^+$ − ^{t}Bu, 46], 276 [Mes*P$^+$, 31], 261 [Mes*P$^+$–CH$_3$, 45], 220 [Mes*PH$^+$–^{t}Bu, 100], 57 [^{t}Bu$^+$, 78].

3.2. Insertion of 1 into P–Si bond of Mes*PHSiMe$'_2$Bu

To a solution of 1 (0.12 g, 0.29 mmol) in 20 ml of hexane was added Mes*PHSiMe$_2$Bu (0.118 g, 0.30 mmol) in THF (20 ml). The mixture became slowly yellow–green and was stirred at room temperature (r.t.) for 36 h. The solvent was removed in vacuum, and the residue was extracted with 40 ml of n-hexane to give 0.10 g of green crystals (2) in 43% yield. Elemental Anal. Found: C, 72.63; H, 9.82; N, 1.76. C$_{49}$H$_{78}$NP$_2$ClSi, Calc.: C, 72.95; H, 9.75; N, 1.74%. IR: 3393 m, 2974 s, 2874 m, 1657 w, 1509w, 1460 s, 1361 w, 1260 s, 1177 m, 1069 s, 911 s, 808 m, 662 m. MS (EI): m/z (fragment, relative intensity) = 806 [M$^+$, 2], 749 [M$^+$ − ^{t}Bu, 15], 691 [M$^+$ − SiMe$'_2$Bu, 5], 528 [M$^+$ − Mes*H$_2$, 2], 472 [M$^+$ − Mes*PH–^{t}Bu, 22], 277 [Mes*PH$^+$, 26], 220 [Mes*PH$^+$–^{t}Bu, 14], 115 [SiMe$'_2$Bu$^+$, 4], 73 [Me$_2$Si=NH$^+$, 100], 57 [^{t}Bu$^+$, 59]. UV (hexane): λ_{max} 222 (ε 63 900), 232 (61 540), 286 (32 920), 334 nm (sh 18 600).

3.3. Dimerization of 1

To a solution of Mes*P=C=NAr (1) (0.12 g, 0.29 mmol) in THF (25 ml) was added anhydrous YCl$_3$ (0.10 g, 0.51 mmol). The mixture became brown immediately and was stirred at r.t. over night. The solvent was removed in vacuum, and 3 was extracted from the resulting residue with n-hexane. Cooling of the concentrated n-hexane solution to $-20°C$ gave 3 as yellow crystals (0.050 g, yield 42%). M.P. 238–240°C. Elemental Anal. Found: C, 72.12; H, 7.98; N, 3.41. Calc. for C$_{50}$H$_{66}$N$_2$P$_2$Cl$_2$: C, 72.53; H, 8.03; N, 3.38%. IR (KBr): 3442 m, 2963 s, 2868 m, 1591 m, 1521 s, 1480 s, 1393 m, 1362 m, 1120 w, 1089 w, 1006 m, 829 m, 612 m, 540 w, 498 w, 464 w, 428 w cm^{-1}. MS (EI): m/z (fragment, relative intensity) = 715 [M$^+$ − Ar, 1.5], 630 [M$^+$ − NAr–^{t}Bu–CH$_3$ + 1, 3.4], 586 [M$^+$ − 2Ar–CH$_4$, 2.0], 494 [M$^+$ − Mes*–^{t}Bu–2CH$_3$, 1.2], 413 [(M/2)$^+$, 32.5], 357 [(M/2)$^+$–^{t}Bu + 1, 35.8], 276 [Mes*P$^+$, 13.5], 261 [Mes*P$^+$–CH$_3$, 30.2], 220 [Mes*PH$^+$–^{t}Bu, 52.1], 111 [Ar$^+$, 14.6], 86 [C$_2$P$_2^+$, 1.2], 57 [^{t}Bu$^+$, 100]. UV (hexane): λ_{max} 218 (ε 11 300), 234 (4 630), 242 nm (4630).

3.4. X-ray crystal structure determination of 1

A suitable single crystal was sealed under argon in a thin-walled glass capillary and mounted on an Enraf–Nonius CAD-4 diffractometer. Lattice patameters were determined from the angular settings of 25 reflections with $13.93 < \theta < 14.81°$. Crystal and data collection parameters are given in Table 1. The intensities were
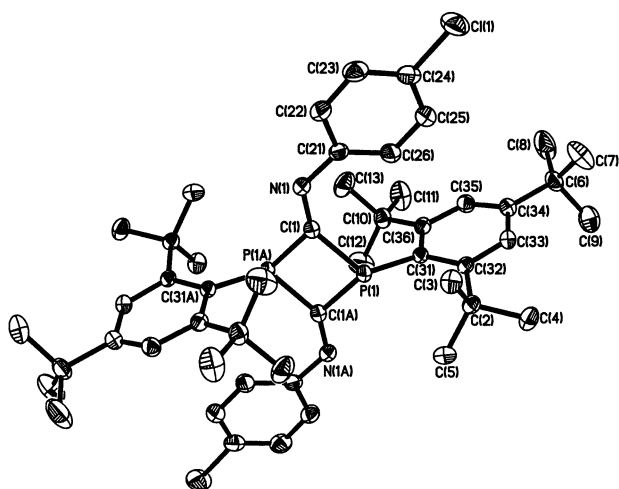
Table 1
Crystal and data collection parameters of **2**, **5**, and **7**

Compound	1	2	3
Formula	$C_{25}H_{33}NPCl$	$C_{49}H_{78}NP_2ClSi$	$C_{50}H_{66}N_2P_2Cl_2$
Molecular weight	413.97	806.65	827.94
Size (mm)	$0.75 \times 0.35 \times 0.20$	$0.30 \times 0.20 \times 0.20$	$0.45 \times 0.35 \times 0.20$
Crystal color	Red–orange	Green	Yellow
Crystal system	Monoclinic	Monoclinic	Triclinic
Space group	$P2_1/n$	$P2_1/n$	$P\bar{1}$
Lattice parameters			
a (Å)	15.200(6)	10.319(3)	9.5349(7)
b (Å)	9.982(6)	23.309(5)	10.3912(8)
c (Å)	15.868(6)	21.41(1)	13.5741(10)
α (°)			69.453(1)
β (°)	99.47(3)	99.64(5)	75.242(1)
γ (°)			70.892(1)
V (Å^3)	2375(3)	5078(3)	1175.0(2)
Z	4	4	1
Diffractometer	Enraf–Nonius CAD4	Rigaku AFC7R	Bruker Smart 1000
Radiation Mo–K$_\alpha$ (λ, Å)	(0.71069)	(0.71073)	(0.71069)
μ (cm^{-1})	2.35	1.92	2.41
Temperature (K)	296	293	296
Type of scan	ω–2θ	ω–2θ	ω–2θ
$2\theta_{max}$ (°)	52	50.0	50.0
Reflections measured	5339	7867	4807
Unique reflections observed	4977	7326($R_{int} = 0.021$)	4045 ($R_{int} = 0.0141$)
Reflections observed	2692 [$I > 3\sigma(I)$]	4359 [$I > 2.5\sigma(I)$]	3550 [$I > 2\sigma(I)$]
Number of variables	253	487	253
Refinement	F	F	F^2
R	0.072	0.049	0.053
R_w	0.083	0.056	0.060
w	$1/\sigma^2(F)$	$1/\sigma^2(F)$	$1/[\sigma^2(F_o^2)+(0.0972P)^2+0.6790P]$ $P = (F_o^2+2F_c^2)/3$
$(\Delta/\sigma)_{max}$	0.06	0.024	0.015
$\Delta\rho_{max}$ (e Å^{-3})	0.32	0.282	0.495

corrected for Lorentz, polarization and absorption effects. The structure was solved by the direct methods (MITHRIL) [35] and refined by full-matrix least squares on *F*. The H-atoms were included in calculated positions with isotropic thermal parameters related to those of the supporting carbon atoms, but were not included in the refinement. All calculations were performed on a Micro VAX 3100 computer.

3.5. X-ray crystal structure determination of *2*

A suitable single crystal of **2** was sealed under N$_2$ in a thin-walled glass capillary. Final lattice parameters were determined from a least-squares refinement using the setting angles of 20 carefully centered reflections in the range $13.48 < 2\theta < 21.44°$. Data were collected on a Rigaku AFC7R diffractometer using the ω–2θ scan technique to a maximum 2θ value of 50.0°. Relevant crystal and data collection parameters are given in Table 1. During the data collection, the intensities of three standard reflections measured every 200 reflections showed linear decay of -1.20%. A linear correction factor was applied. The intensities were corrected for Lorentz, polarization and absorption effects.

The structure was solved by direct methods [36] and expanded using Fourier techniques [37]. The nonhydrogen atoms were refined anisotropically. Hydrogen atoms were included but not refined. The positional parameters for the most reasonable model were fixed for the final least-squares cycles and the isotropic temperature factors allowed to vary. The final cycle of full-matrix least-squares refinement was based on 4359 observed reflections [$I > 2.50\ \sigma(I)$] and 487 variable parameters and converged to the final values of $R = 0.057$ and $R_w = 0.070$. All calculations were performed using the TEXSAN crystallographic software package of Molecular Structure Corporation [38].

3.6. X-ray crystal structure determination of *3*

A yellow crystal of **3** was handled as described above for **1**. Data were collected on a Bruker Smart 1000 diffractometer using the ω–2θ scan technique to a maximum 2θ value of 50.0°. Relevant crystal and data collection parameters are given in Table 1. The intensities were corrected for Lorentz, polarization and absorption effects.

The structure was solved by direct methods and expanded using Fourier techniques. Refinement on F^2 for all reflections, except for **3** with very negative F^2 or flagged by the user for potential systematic errors. The observed criterion of $F^2 > 2\sigma(F^2)$ is only used for calculating R-factors etc. and is not relevant to the choice of reflections for refinement. All calculations were performed using the SHELXL crystallographic software package of Molecular Structure Corporation [39].

4. Supplemental Material

Crystallographic data for the structural analysis has been deposited with the Cambridge Crystallographic Data Centre, CCDC nos. 139772, 139773, 139774 for compounds **1**, **2** and **3**. Copies of this information may be obtained free of charge from The Director, CCDC, 12 Union Road, Cambridge, CB2 1EZ, UK (fax: + 44-1223-336033; e-mail: deposit@ccdc.cam.ac.uk or www: http://www.ccdc.cam.ac.uk).

Acknowledgements

References

[1] J.F. Nixon, Chem. Rev. 88 (1988) 1327.
[2] R. Appel, F. Knoll, Adv. Inorg. Chem. 33 (1989) 259.
[3] T. Niitsu, N. Inamoto, K. Toyota, M. Yoshifuji, Bull. Chem. Soc. Jpn. 63 (1990) 2726.
[4] M.A. David, S.N. Paisner, D.S. Glueck, Organometallics 14 (1995) 17.
[5] J.B. Alexander, D.S. Glueck, G.P.A. Yap, A.L. Rheingold, Organometallics 14 (1995) 3603.
[6] A.H. Cowley, B. Pellerin, J.L. Atwood, S.G. Bott, J. Am. Chem. Soc. 112 (1990) 6734.
[7] H. Ranaivonjatovo, H. Ramdane, H. Gornitzka, J. Escudié, J. Satgé, Organometallics 17 (1998) 1631.
[8] H. Ramdane, H. Ranaivonjatovo, J. Escudié, Organometallics 15 (1996) 3070.
[9] M.A. David, J.B. Alexander, D.S. Glueck, G.P.A. Yap, L.M. Liable-Sands, A.L. Rheingold, Organometallics 16 (1997) 378.
[10] R. Appel, C. Behnke, Z. Anorg. Allg. Chem. 555 (1987) 28.
[11] D.H. Gihson, Chem. Rev. 96 (1999) 2063.
[12] J. Baker, M. Kilner, Coord. Chem. Rev. 133 (1994) 219.
[13] P. Braunstein, D. Nobel, Chem. Rev. 89 (1989) 1927.
[14] C.C. Chang, J.H. Chen, B. Srinivas, M.Y. Chiang, G.H. Lee, S.M. Peng, Organometallics 16 (1997) 4980 and references therein.
[15] R. Appel, P. Folling, L. Krieger, M. Riray, F. Knoch, Angew. Chem. Int. Ed. Engl. 23 (1984) 970.
[16] O.I. Kolodiazhnyi, Tetrahedron Lett. 23 (1982) 4933.
[17] M. Yoshifuji, K. Toyota, K. Shibayama, N. Inamoto, Tetrahedron Lett. 25 (1984) 1809.
[18] T. Vincent, P.J. Wheatley, J. Chem. Soc. Perkin 2 (1972) 687.
[19] M. Yoshifuji, K. Shibayama, K. Toyota, N. Inamoto, K. Hirotsu, Y. Odagaki, T. Higuchi, S. Nagase, Polyhedron 7 (1988) 2213.
[20] H.H. Karsch, H.U. Reisacher, G. Müller, Angew. Chem. Int. Ed. Engl. 23 (1984) 618.
[21] R. Appel, F. Knoll, I. Ruppert, Angew. Chem. Int. Ed. Engl. 20 (1981) 731.
[22] M. Yoshifuji, K. Toyota, I. Matsuda, T. Niitsu, N. Inamoto, K. Hirotsu, T. Higuchi, Tetrahedron 44 (1988) 1363.
[23] M. Yoshifuji, I. Shima, N. Inamoto, K. Hirotsu, T. Higuchi, J. Am. Chem. Soc. 103 (1981) 4587.
[24] N. Tokitoh, Y. Arai, R. Okazaki, S. Nagase, Science 277 (1997) 78.
[25] N. Tokitoh, Y. Arai, T. Sasamori, R. Okazaki, S. Nagase, H. Uekusa, Y. Ohashi, J. Am. Chem. Soc. 120 (1998) 433.
[26] S. Nagase, S. Suzuki, T. Kurakake, J. Chem. Soc. Chem. Commun. (1990) 1724.
[27] B. Twamley, C.D. Sofield, M.M. Olmstead, P.P. Power, J. Am. Chem. Soc. 121 (1999) 3357 and references therein.
[28] J. Brown, Acta Crystallogr. 21 (1966) 146.
[29] G. Becker, H. Riffel, W. Uhl, H.J. Wessely, Z. Anorg. Allg. Chem. 534 (1986) 31.
[30] W.J. Evans, C.A. Seibel, J.W. Ziller, R.J. Doedens, Organometallics 17 (1998) 2103.
[31] W.J. Evans, K.J. Forrestal, J.W. Ziller, J. Am. Chem. Soc. 120 (1998) 9273.
[32] W. Egan, R. Tang, G. Zon, K. Mislow, J. Am. Chem. Soc. 93 (1971) 6205.
[33] F. Mathey, Coord. Chem. Rev. 88 (1988) 429.
[34] A.H. Cowley, N.C. Norman, M. Pakulski, Inorg. Synth. 17 (1990) 235.
[35] C.J. Gilmore, MITHRIL, A Computer Program for the Automatic Solution of Crystal Structures from X-ray Data, University of Glasgow, Glasgow, 1983.
[36] G.M. Sheldrick, SHELXS-86, in: G.M. Sheldrick, C. Kruger, R. Goddard (Eds.), Crystallographic Computing, vol. 3, Oxford University Press, Oxford, 1986, pp. 175–189.
[37] P.T. Beurskens, G. Admiraal, G. Beurskens, W.P. Bosman, S. Garcia-Granda, R.O. Gould, J.M.M. Smits, C. Smykalla, DIRDIF-92: The DIRDIF program system, in: Technical Report of the Crystallography Laboratory, University of Nijmegen, Netherlands, 1992.
[38] TEXSAN: Crystal Structure Analysis Package, Molecular Structure Corporation, 1985 and 1992.
[39] G.M. Sheldrick, SHELXL-97, Program for the refinement of crystal structure, University of Göttingen, Germany, 1997.